

measurements), and this may represent a major breakthrough for molecular materials. This provides the possibility of molecular bistability in which the magnetization becomes 'frozen' in one of two potential wells at low temperature. If a means is found of properly addressing individual clusters it might then be possible to store information at the molecular level—albeit at temperatures no greater than about 4 K in this case. □

Received 21 June; accepted 13 July 1993.

1. Gunther, L. *Phys. Wld.* **3**, 28–31 (1990).
2. Awschalom, D. D., Di Vincenzo, D. P. & Smyth, J. F. *Science* **258**, 414–416 (1992).
3. Stamp, P. C. E., Chudnovsky, E. M. & Barbara, B. *Int. J. mod. Phys.* **B6**, 1355–1473 (1992).
4. McMichael, R. D., Shull, R. D., Swartzendruber, L. J., Bennett, L. H. & Watson, R. E. *J. magn. Mater.* **111**, 29–33 (1992).
5. Papaefthymiou, G. C. *Phys. Rev.* **B46**, 10367–10375 (1992).
6. Kahn, O., Pei, Y. & Journaux, Y. in *Inorganic Materials* (eds Bruce, D. W. & O'Hare, D.) 59–114 (Wiley, Chichester, 1992).
7. Lis, T. *Acta crystallogr.* **B36**, 2042–2046 (1980).
8. Caneschi, A. et al. *J. Am. chem. Soc.* **113**, 5873–5874 (1991).
9. Sessoli, R. et al. *J. Am. chem. Soc.* **115**, 1804–1816 (1993).
10. Brown, W. F. *Jr Phys. Rev.* **130**, 1677–1686 (1963).
11. Jacobs, I. S. & Bean, C. P. in *Magnetism* Vol. 3 (eds Rado, G. T. & Suhl, H.) 271–348 (Academic, New York, 1963).

ACKNOWLEDGEMENTS. We thank the Italian MURST and the Progetto Finalizzato 'Materiali Speciali per Tecnologie Avanzate' for financial support, and J. L. Tholence and M. Guillot for discussions and the experimental facilities they provided. M.A.N. acknowledges a scholarship from CNPq (Brasil) during part of this work.

Correlations between climate records from North Atlantic sediments and Greenland ice

Gerard Bond*, Wallace Broecker*,
Sigfus Johnsen†‡, Jerry McManus*,
Laurent Labeyrie§, Jean Jouzel||¶
& Georges Bonani#

* Lamont-Doherty Earth Observatory of Columbia University, Palisades, New York 10964, USA

† The Niehls Bohr Institute, Department of Geophysics, University of Copenhagen, Haraldsgade 6, DK-2200, Copenhagen N, Denmark

‡ Science Institute, Department of Geophysics, University of Iceland, Dunghaga 3, IS-107 Reykjavik, Iceland

§ CFR Laboratoire mixte CNRS-CEA, Domaine du CNRS, 91198, Gif-sur-Yvette, Cedex, France

|| Laboratoire de Modélisation du Climat et de l'Environnement, CEA/DSM, CE Saclay 91191, France

¶ Laboratoire de Glaciologie et Géophysique de l'Environnement, CNRS, BP96, 38402 St. Martin d'Hères Cedex, France

Institute für Mittelenergiephysik, ETH Honggerberg, CH-8093 Zurich, Switzerland

OXYGEN isotope measurements in Greenland ice demonstrate that a series of rapid warm–cold oscillations—called Dansgaard–Oeschger events—punctuated the last glaciation¹. Here we present records of sea surface temperature from North Atlantic sediments spanning the past 90 kyr which contain a series of rapid temperature oscillations closely matching those in the ice-core record, confirming predictions that the ocean must bear the imprint of the Dansgaard–Oeschger events^{2,3}. Moreover, we show that between 20 and 80 kyr ago, the shifts in ocean–atmosphere temperature are bundled into cooling cycles, lasting on average 10 to 15 kyr, with asymmetrical saw-tooth shapes. Each cycle culminated in an enormous discharge of icebergs into the North Atlantic (a 'Heinrich event'^{4,5}), followed by an abrupt shift to a warmer climate. These cycles document a previously unrecognized link between ice sheet behaviour and ocean–atmosphere temperature changes. An important question that remains to be resolved is whether the cycles

are driven by external factors, such as orbital forcing, or by internal ice-sheet dynamics.

Measurements of $\delta^{18}\text{O}$ in the new GRIP ice core from Summit, Greenland provide the first record of air temperatures over the ice cap spanning the last 250 kyr¹. We have correlated the last 90 kyr of that record with a proxy of sea surface temperature in two North Atlantic cores, DSDP site 609 and V23-81 (Fig. 1). The proxy of sea surface temperature is the abundance of *Neogloboquadrina pachyderma* (s.), a planktic foraminifera which lives in waters $<10^\circ\text{C}$ and comprises about 95% of the fauna at summer temperatures $<5^\circ\text{C}$ ^{6,7}. Correlation among the foraminiferal records is constrained by depths of Heinrich events and AMS ¹⁴C measurements (Figs 2, 3; and Table 1). Bioturbation of sediment is so low in both cores that we were able to sample at a resolution of 300–500 yr. In addition, by avoiding burrows and other sediment disturbances in V23-81, our new AMS ¹⁴C ages have no reversals, a problem that hampered previous radiocarbon dating of that core⁸. We note that ¹⁴C measurements in V23-81 and V30-101k revise previous age estimates for Heinrich events 3 and 4 (refs 4, 5) from 28 to 27 kyr BP (before present) and from 41 to 35.5 kyr, respectively (Table 1).

A conspicuous feature common to both the ice and ocean records enabled us to correlate them in spite of their uncertain chronologies. That feature is a bundling of the millennial-scale Dansgaard–Oeschger cycles into longer cooling cycles, each terminated by an abrupt shift from cold to warm temperatures (Fig. 3). We matched the records at the points of abrupt temperature shifts and then 'stretched' the ice-core record linearly until the points were aligned. That alignment is justified by the fact that at the latitudes of our cores (50 – 54°N), shifts in sea surface temperatures must be in phase with air temperature changes above Greenland, especially at the sharp terminations of Dansgaard–Oeschger cycles.

What makes the correlation convincing is that down core, the changes in shapes and internal structures of the longer cycles is nearly the same in all the records (Fig. 3). The stepped pattern of cooling between the Younger Dryas (YD) and ice-core interstadial 1e is closely matched in V23-81, a pattern recognized previously in this core^{8,9} and in the Norwegian Sea¹⁰. Between ice-core interstadials 1e and 2, a 'W'-like pattern with superimposed, short oscillations appears in the ice and sediment,

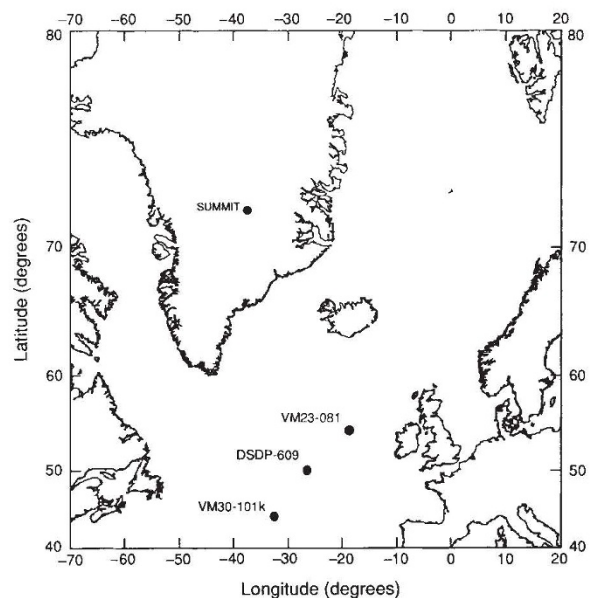


FIG. 1 Locations of the Summit ice core and the deep-sea cores described in this work.

especially in V23-81. Two short interstadials just below the 'W' also appear in V23-81. Between ice-core interstadials 2 and 20 are five asymmetrical cycles, each containing progressively cooler interstadials and culminating in a prominent cold stadial. Much of the structure within these cycles also appears in the foraminiferal records. Finally, the two oscillations on the stage 4/5 boundary and the cooling within marine stage 5b are present in all three records¹¹.

The only direct confirmation of our correlation so far comes from the upper parts of the records where ice-core dating and radiocarbon to calendar age conversions are reasonably well established¹²⁻¹⁴. There, except for the oldest layer, calendar ages of correlated ice and sediment differ by no more than a few hundred years (Table 1, Fig. 3). Two other tests yet to be performed are the depths predicted for marine Ash layers I and II in the ice core (Figs 2, 3).

Our timescale is constrained by ¹⁴C dating for the past ~35,500 years. Below the level of ¹⁴C dating in V23-81 we assigned ages from DSDP site 609 to H5 (50 kyr), to H6 (66 kyr) and to the sharp peak in stage 5b (84.4 kyr) and then interpolated linearly between them. To date the level below 5b in V23-81, we extrapolated the sedimentation rate between H6 and

the sharp peak in 5b. Whereas our timescale is broadly consistent with previous dating of the ice core¹ and with the SPECMAP chronology¹⁵, we emphasize that it is not intended to be an age model for the ice core. Conversion of ¹⁴C ages to calendar ages is uncertain, especially beyond ~20 kyr yr, and sedimentation rates in the marine cores are probably not linear. In fact, the spacing of the ice-core depth intervals should increase steadily down core, and the deviation from that spacing below about 2,200 m (Fig. 3) may be an artefact of changes in sedimentation rates in DSDP site 609.

Our new findings are the strongest evidence so far that Dansgaard-Oeschger cycles are imprinted in the marine sediments of the North Atlantic. The temperature shifts, especially in V23-81, occur on millennium timescales and have asymmetric shapes, sharp boundaries and strong amplitudes (up to a change in temperature of ~5 °C), features which characterize the Dansgaard-Oeschger cycles. A number of the Dansgaard-Oeschger cycles even appear to have direct correlatives in the marine records (Fig. 3). Clearly, for at least 80 kyr the atmosphere and ocean surface were a coupled system, repeatedly undergoing massive reorganizations on timescales of centuries or less. At the abrupt cold-to-warm shifts that terminate

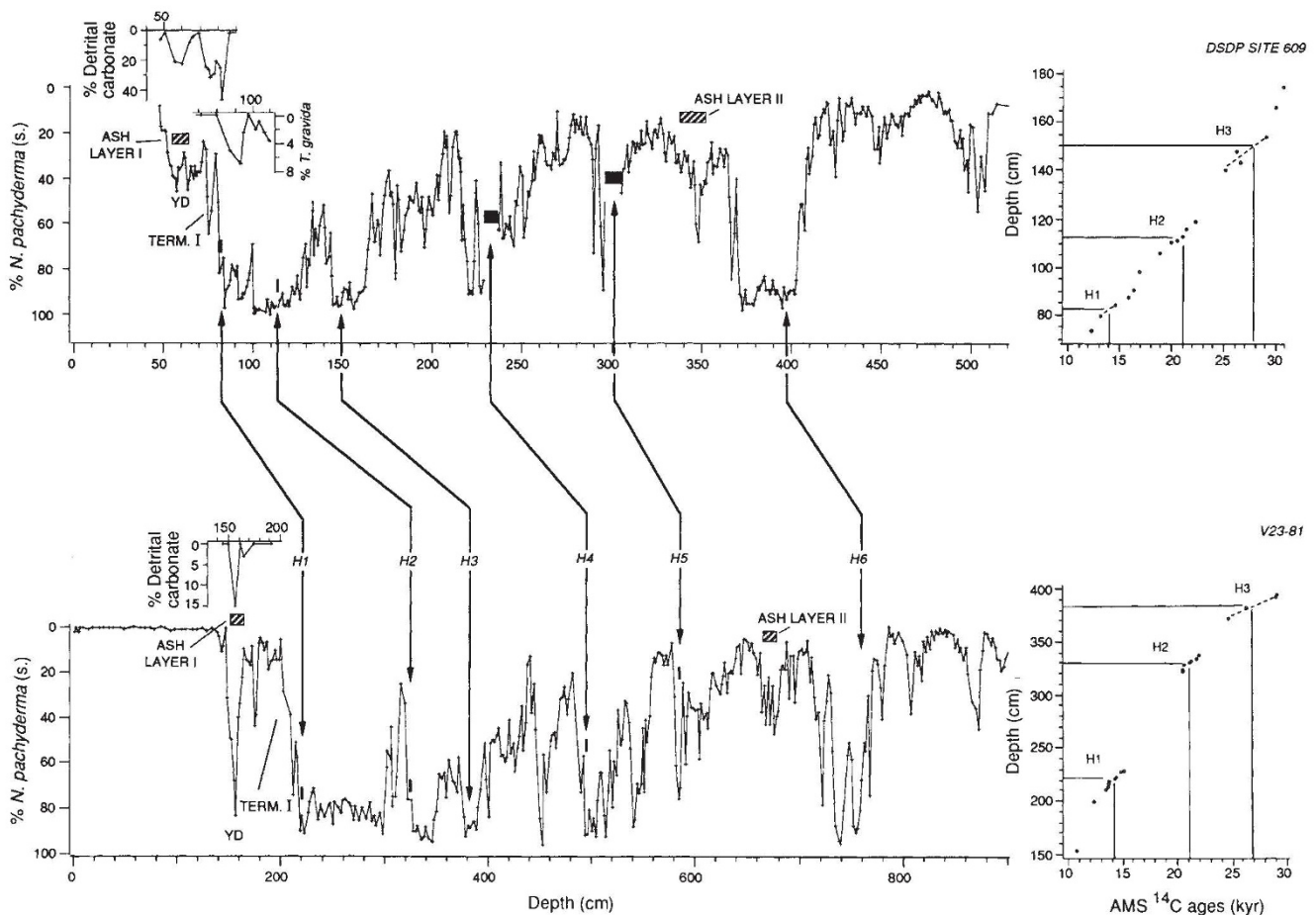


FIG. 2 Abundances of *N. pachyderma* (s.) in two North Atlantic cores, DSDP site 609 (top) and V23-81 (bottom). Samples from DSDP site 609 are from every centimetre; in V23-81, samples are from every 2 cm. Also shown for both sites are new measurements of % detrital carbonate (inset, top and bottom) across the levels of the Younger Dryas (YD) event, demonstrating large discharges of icebergs at that time, presumably from the Laurentide ice sheet. The % of *T. gravida*, a polar diatom (inset, top), indicates a warm-cold oscillation within isotope stage 2 at DSDP site 609. Depths of Ash Layer I and II are based on peak concentrations of the rhyolitic glass that defines those horizons.

Heinrich events, shown as H1 to H6, are brief intervals of increased discharge of icebergs and reduced foraminiferal fluxes that serve as excellent markers for correlation among the marine cores⁴. The AMS ¹⁴C ages to the right of the records are listed in Table 1. In both cores, detrital carbonate-bearing layers within Heinrich deposits are indicated by the black bars (Fig. 2). At DSDP site 609 the detrital carbonate-rich layers at H2, H4 and H5 accumulated nearly instantaneously⁴ and are so thick that they must be removed before constructing the time series. In core V23-81, none of the layers containing detrital carbonate are thick enough to require removal.

Dansgaard-Oeschger cycles (Fig. 2), rates of change in ocean temperatures must have been nearly the same as in the ice core; that is, several degrees within decades^{9,13,16,17}. The large amplitudes and high rates of these temperature shifts are independent of ice volumes, occurring during deglaciation, during the glacial maximum, during the warmer isotope stage 3 and even during the inception of large ice sheets at the stage 4/5 boundary.

Perhaps the most important finding of our study is evidence of an unexpectedly close relation between the ice-core temperature cycles and one of the most prominent features of North Atlantic records, the Heinrich events. Heinrich events occur during times of sea surface cooling, reduced fluxes of foraminifera and brief, exceptionally large discharges of icebergs from the Laurentide ice sheet that left conspicuous layers of detrital carbonate in deep sea sediment^{4,5,18}. Accompanying these events were large decreases in planktic $\delta^{18}\text{O}$ (Fig. 3), evidence of lowered surface salinities probably caused largely by melting of the drifting ice⁴.

Our correlation demonstrates that the iceberg discharges and salinity drops must have occurred during times of particularly cold stadials (Fig. 3). Supporting this is evidence that H1 has the same calendar age, within error, as the younger cold cycle in the 'W' (cycle a, Fig. 3, Table 1). In addition, the Younger Dryas, which unquestionably correlates with a prominent stadial in the ice core (Fig. 3), has features in common with Heinrich events. During the Younger Dryas, North Atlantic sea surface temperatures dropped¹⁹, salinities decreased²⁰, and Laurentide ice advanced through Hudson Strait, depositing detrital carbonate-bearing sediment in the Labrador Sea²¹. We have now found elevated percentages of detrital carbonate in sediments of Younger Dryas age (Fig. 2), indicating that, just as during the Heinrich events, icebergs drifted from the Labrador Sea far into the North Atlantic⁴. We note that the match of Heinrich events to cold stadials confirms our earlier suggestion that Heinrich events formed during periods of extreme atmospheric cooling⁴.

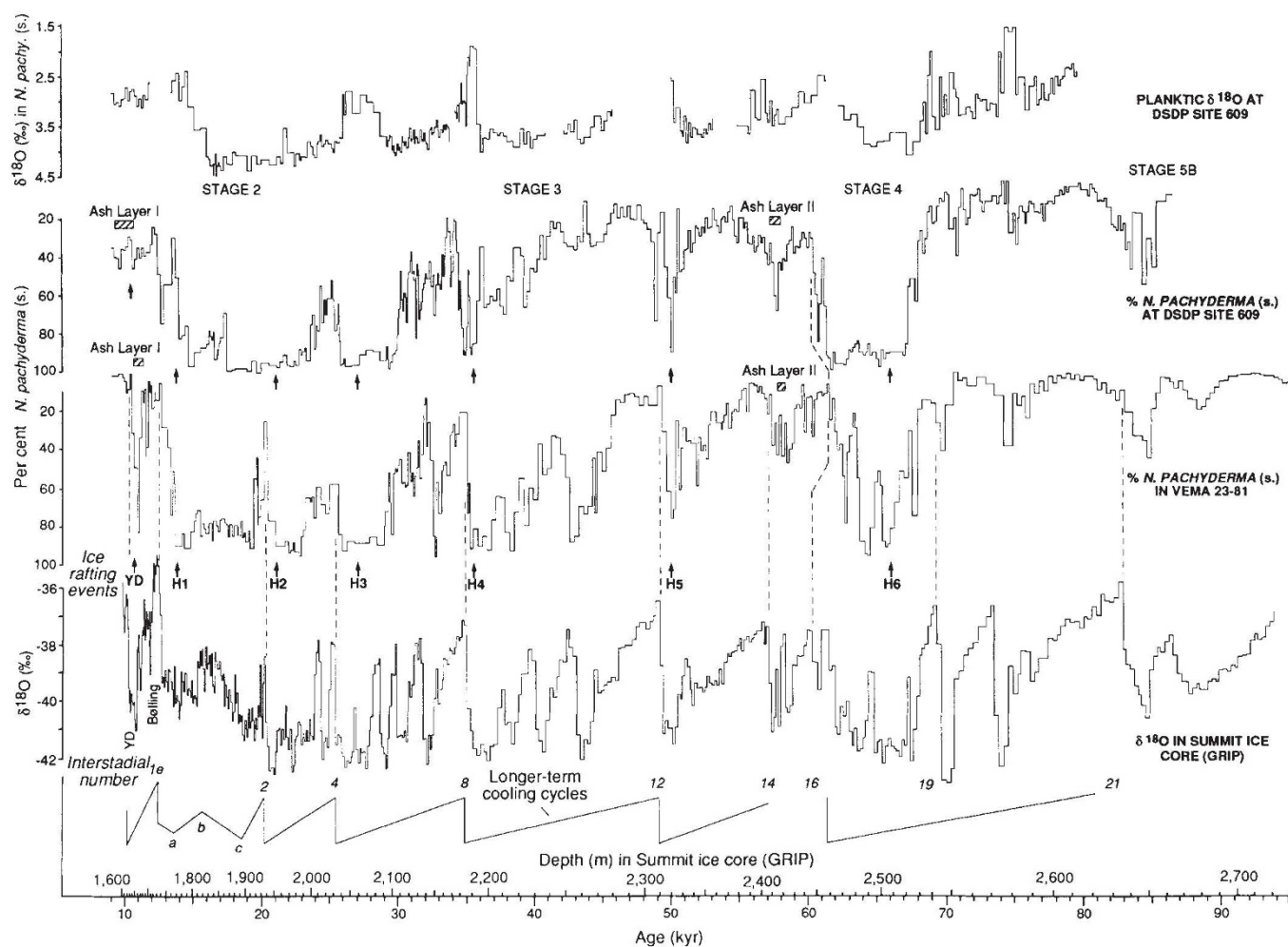


FIG. 3 Our correlation of the foraminiferal records from DSDP site 609 and V23-81 with the new $\delta^{18}\text{O}$ record from GRIP, Summit, Greenland. (Note that the timescale is not an age model for the ice core.) The interstadial numbers in the ice-core record are from the numbering system in ref. 1. Also shown are the longer-term cooling cycles, defined by bundling of millennium scale cycles (Dansgaard-Oeschger cycles) and abrupt shifts to markedly warm interstadials. The dashed lines were used as tie points for matching the ice-core and marine records. The bend in the tie point corresponding to interstadial 16 probably reflects a small decrease in the sedimentation rate at this depth in V23-81 relative to DSDP 609. See text for construction of the timescale. At the top of the figure is the planktic $\delta^{18}\text{O}$ measured in *N. pachyderma* (s.)⁴.

The heavy arrows mark the locations of the IRD peaks within the Heinrich events (H1 to H6) and the peak concentrations of detrital carbonate IRD in the Younger Dryas event. The boxes filled with slanted lines are the levels of Ash Layer I and II in the marine cores; the correlatives of these layers in the ice core should occur at depths of ~1,630 m (Ash Layer I) and ~2,426 m (Ash Layer II). It should be noted that the short cooling cycle at about 13,000 ^{14}C yr BP in DSDP site 609, a contemporaneous decrease in the rate of warming in V23-81 and the cold peak containing H1 in V23-81 between 14,000 and 15,000 ^{14}C yr were not recognized previously^{4,5}. These revisions are a consequence of our new foraminiferal measurements in both cores and the improved ^{14}C dating in V23-81.

TABLE 1 Radiocarbon ages for cores DSDP 609, V23-81, and V30-101k

Core	Depth (cm)	Corrected age* (yr)	Error (±yr)	Core	Depth (cm)	Corrected age* (yr)	Error (±yr)
DSDP 609	73–75	12,350*	220	V23-81	154–155	10,900‡	140
DSDP 609 (G.b.)	79–81	13,250*	090	V23-81	198–199	12,320‡	220
DSDP 609	84–85	14,590*	230	V23-81	210	13,440§	120
DSDP 609	87–88	15,960*	240	V23-81	213	13,600§	120
DSDP 609	90–91	16,360*	150	V23-81	217	13,610§	100
DSDP 609	98–99	16,960*	120	V23-81	219	13,630§	100
DSDP 609	105–107	18,940*	220	V23-81	221	14,150§	110
DSDP 609	110–111	19,970*	330	V23-81	223	14,330§	100
DSDP 609	111–112	20,550*	260	V23-81	227	14,770§	110
DSDP 609	112–113	21,110*	220	V23-81	229	15,040§	110
DSDP 609	115–116	21,370*	220	V23-81	321	20,420§	180
DSDP 609	118–120	22,380*	340	V23-81	323	20,470§	160
DSDP 609 (G.i.)	139–141	25,260*	440	V23-81	327	20,570§	180
DSDP 609	147–149	26,170*	310	V23-81	329	20,990§	170
DSDP 609	153–155	29,170*	660	V23-81	331	21,210§	170
DSDP 609	166–167	30,080*	680	V23-81	333	21,700§	180
DSDP 609 (G.i.)	174–176	30,720*	730	V23-81	337	21,960§	190
V30-101k	56–57	23,570§	210	V23-81	371	24,680§	200
V30-101k H4† (80 cm)–	70	33,250§	510	V23-81	381	26,270§	260
V30-101k	85	36,570§	650	V23-81	391	28,980§	320
				V23-81	393	29,050§	310

Ages of interstadial 1e and the 'W' (levels a, b and c) in Fig. 3

Level	¹⁴ C age (yr) in marine cores	Calendar age (yr) in marine cores	Ice core age¶
1e	12,300	14,300	14,500
a	13,550	16,000	16,400
b	15,400	18,440	18,800
c	18,400	21,970	21,070

* Corrected for assumed 400-yr difference between surface-water carbon and atmospheric carbon; G.b. = analyses on *G. bulloides*; G.i. = analyses on *G. inflata*; all other analyses done on *N. pachyderma* (s).

† H4 in V30-101k is Heinrich layer 4 (this layer was initially identified as H3 in ref. 4; subsequent analyses of that core now demonstrate that it is H4).

‡ ref. 8.

§ AMS ¹⁴C ages from analyses done at ETH-Zurich for this work.

|| ref. 14.

¶ ref. 12.

* ref. 4.

It is also significant that except for H1, the Heinrich events, and the Younger Dryas ice rafting event as well, consistently occur near the ends of the bundled Dansgaard-Oeschger cycles that constrain much of our correlation (Fig. 3). The bundles form a series of saw-tooth shaped cycles, each defined by a succession of progressively cooler interstadials (Fig. 3), probably reflecting a progressive strengthening of the polar cell. Each cycle culminates in a prolonged cold period (stadial) during which a Heinrich event occurs. Following the stadial is a rapid termination-like shift to a prominent warm interstadial marking the beginning of the next cycle (Fig. 3). This complex pattern, known previously only from deglacial records^{8, 10}, persists through almost all of the last glaciation, the only exceptions being the intervals through the 'W' and stage 5b.

The series of saw-tooth shaped cooling cycles is clearly a fundamental structure of the atmosphere and sea-surface records, and must bear a close relation to the Heinrich events and the repeated, massive collapses of the Laurentide ice sheets. With the evidence in hand we cannot be certain whether the cooling cycles were caused entirely by internal oscillations of the ice sheet²², or whether they reflect a mode of climate forcing that caused ice sheets to grow, culminating each time in a prolonged, cold stadial, ice-sheet instability and massive calving. If internal oscillations of the ice sheet are sole mechanisms, they must have operated during times such as the Younger Dryas when ice volumes had decreased. We note however, that because H1 comes at the end of a different type of cycle, the 'W', its relation to

climatic and ice-sheet mechanisms may well have been different from that of the others.

The abrupt warmings that followed the Heinrich events and that caused the asymmetry of the cooling cycles, on the other hand, could have been a direct consequence of the ice. Collapse of the ice sheet and landward retreat of ice streams after each event must have reduced the flux of icebergs to the open ocean. The resulting increase in surface salinity could have been large enough to strengthen thermohaline circulation, rapidly bringing heat into the North Atlantic. If so, that further supports our suggestion⁴ that iceberg meltwater strongly influenced the North Atlantic's thermohaline circulation during glaciation.

Whatever their origin, the series of asymmetric cooling cycles and the prominent warmings that terminate them are so conspicuous in the atmospheric and ocean surface records of the North Atlantic that they must be imprinted in other records from the last glaciation. In fact, a series of prominent cycles on timescales of several thousands of years appears within marine stage 3 in summer sea surface temperature estimates from other North Atlantic deep-sea cores^{23, 24}, in the Grand Pile pollen record²⁵, and in high-resolution benthic $\delta^{18}\text{O}$ records from core V19-30 in the eastern equatorial Pacific²⁶. Perhaps the sea-level highstands demarked in the flights of the marine terraces of the last glaciation²⁷ are the consequence of massive ice sheet collapses during Heinrich events and the warmings at the ends of the cycles. To test these ideas, however, will require the analysis of records with more precise chronologies and at much higher

resolution than has been attempted to date.

Our new findings still leave unexplained the Dansgaard-Oeschger oscillations in air temperature over Greenland that punctuate the intervals between the Heinrich events. Perhaps, as we suggested earlier³, these reflect the salt-induced ocean circulation oscillations caused by an interaction between the ocean heat-pump and the Scandinavian ice sheets. Although many questions remain unanswered, our correlation of the Heinrich events so prominent in the ice cores with the more frequent Dansgaard-Oeschger events in the ice cores brings us significantly closer to understanding the complex link between ice-sheet dynamics and ocean operation. □

Received 21 April; accepted 16 July 1993.

- Dansgaard, W. *et al.* *Nature* **364**, 218–220 (1993).
- Broecker, W. S. *et al.* *Quat. Res.* **30**, 1–6 (1988).
- Broecker, W. S., Bond, G. & Klas, M. *Paleoceanogr.* **5**(4), 469–477 (1990).
- Bond, G. *et al.* *Nature* **360**, 245–249 (1992).
- Broecker, W. S., Bond, G., Klas, M., Clark, E. & McManus, J. *Clim. Dynamics* **6**, 265–273 (1992).
- Bé, A. W. H. & Toldertund, D. S. *Micropaleontology of Oceans* (eds Funnell, B. M. & Riedel, W. R.) 105–149 (Cambridge Univ. Press, 1971).
- Kellogg, T. B. *Boreas* **9**, 115–137 (1980).
- Broecker, W. S. *Paleoceanogr.* **3**(1), 1–19 (1988).
- Lehman, S. J. & Keigwin, L. D. *Nature* **356**, 757–762 (1992).
- Karpuz, N. C. & Jansen, E. *Paleoceanogr.* **7**(4), 499–520 (1992).
- Bond, G., Broecker, W., Lotti, R. & McManus, J. in *Start of a Glacial* (eds Kukla, G. J. & Went, E.) 185–205 (Springer, Berlin, 1992).

- Johnsen, S. J. *et al.* *Nature* **359**, 311–313 (1992).
- Alley, R. B. *et al.* *Nature* **362**, 527–529 (1993).
- Bard, E., Arnold, M., Fairbanks, R. G. & Hamelin, B. *Radiocarbon* **3**(1), 191–199 (1993).
- Martinson, D. G. *et al.* *Quat. Res.* **27**, 1–29 (1987).
- Dansgaard, W., White, J. W. C. & Johnsen, S. J. *Nature* **339**, 532–533 (1989).
- Taylor, K. C. *et al.* *Nature* **361**, 432–436 (1993).
- Heinrich, H. *Quat. Res.* **29**, 142–152 (1988).
- Ruddiman, W. F. & McIntyre, A. *Paleogeogr. Palaeoclimatol. Palaeoecol.* **35**, 145–214 (1981).
- Duplessy, J.-C., Labeyrie, L., Juillet-LeClerc, A. & Duprat, J. in *The Last Deglaciation: Absolute and Radiocarbon Chronologies* (eds Bard, E. & Broecker, W. S.) 201–208 (Springer, Berlin, 1992).
- Andrews, J. T., Tedesco, K., Briggs, W. M. & Evans, L. W. *Can. J. Earth Sci.* (in the press).
- MacAyeal, D. R. *Nature* **359**, 29–32 (1992).
- Ruddiman, W. F. in *Northern America and Adjacent Oceans during the Last Deglaciation: The Geology of North America* (eds Ruddiman, W. F. & Wright, H. E. Jr) 137–154 (Geol. Soc. of Am, Boulder, 1987).
- Sancetta, C., Imbrie, J. & Kipp, N. G. *Quat. Res.* **3**, 110–116 (1973).
- Woillard, G. & Mook, W. G. *Science* **215**, 159–161 (1982).
- Shakleton, N. J., Imbrie, J. & Hall, M. A. *Earth planet. Sci. Lett.* **65**, 233–244 (1983).
- Bloom, A. L., Broecker, W. S., Chappell, J. M. A., Matthews, R. K. & Mesolella, K. J. *Quat. Res.* **4**, 185–205 (1974).

ACKNOWLEDGEMENTS. This research was supported in part by grants from the US National Science Foundation (NSF) and NOAA. The ice-core data are from the Greenland Ice Core Project (GRIP) organized by the European Science Foundation. The measurement of planktic $\delta^{18}\text{O}$ was supported by the French CNRS, CEA and CEE(EPOCH). We thank the Ocean Drilling Program for permission to sample cores from DSDP site 609. Support for the core collection of Lamont-Doherty Geological Observatory is provided by the NSF and the Office of Naval Research. We thank C. Sancetta for providing her unpublished diatom data from DSDP site 609. We also thank G. Denton, E. Jansen, S. Leyman, D. MacAyeal and P. Mayewski for comments on the manuscript.

Sharpness of upper-mantle discontinuities determined from high-frequency reflections

H. M. Benz* & J. E. Vidale†

* US Geological Survey, Golden, Colorado 80401, USA

† US Geological Survey, Menlo Park, California 94025, USA

AN understanding of the nature of seismic discontinuities in the Earth's upper mantle is important for understanding mantle processes: in particular, the amplitude and sharpness of these discontinuities are critical for assessing models of upper-mantle phase changes and chemical layering. So far, seismic studies aimed at determining the thickness and lateral variability of upper-mantle discontinuities have yielded equivocal results, particularly for the discontinuity at 410 km depth^{1,2}. Here we present short-period (0.8–2.0 s) recordings of upper-mantle precursors to the seismic phase P'P' (PKPPK) from two South American earthquakes recorded by the ~700-station short-period array in California. Our results show that the 410- and 660-km discontinuities beneath the Indian Ocean are locally simple and sharp, corresponding to transition zones of 4 km or less. These observations pose problems for mineral physics models^{3–5}, which predict a transitional thickness greater than 6 km for the peridotite to β -spinel phase transition. In contrast to the results of long-period studies^{6,7}, we observe no short-period arrivals from near 520 km depth.

Experimental and thermodynamic studies^{3–5,8} suggest that a peridotite to β -spinel phase transition near 410 km depth occurs over a range of 6–19 km, whereas a δ -spinel to perovskite and magnesiowüstite phase transition near 660 km depth occurs over a smaller range of 1–10 km. Some argue⁹, on the basis of seismic observations of sharp discontinuities, that the upper mantle is chemically stratified, while others¹⁰ propose a non-equilibrium phase transformation as a possible explanation for the observation of sharp boundaries. Topographic variations of ± 20 km on the 660-km discontinuity¹¹ favour phase transitions. A recent seismic investigation¹² of near-receiver converted phases argues for a transitional 660-km discontinuity (20–30 km in thickness)

and a sharp 410-km discontinuity. These results contradict previous studies of P'P' precursors^{1,13–15} that observed a simple and sharp 660-km discontinuity. A paucity of high-frequency P'P' precursors from near 410 km depth^{1,2,15} has made it difficult to determine the sharpness of this discontinuity. This leads some² to suspect defocusing effects due to topography or lateral variations in transitional thickness. Previous studies^{1,2,15} have been limited in their ability to characterize the lateral variability in the sharpness of the 410-km discontinuity, primarily owing to small array apertures and sparseness of observations.

From our survey of large-magnitude South American earthquakes ($M > 6.2$), all clear P'P' arrivals were accompanied by short-period (0.8–2.0 s) P'660P' precursors, implying that the 660-km discontinuity beneath the Indian Ocean is simple and sharp, consistent with previous P'P' observations^{1,13–15}. The dense sampling and large aperture of our array (Fig. 1a), combined with the two closely spaced South American earthquakes leads to unprecedented sampling of the upper mantle, enabling us to show the best evidence to date that the 410-km discontinuity is locally as sharp as 4 km thick, but varies laterally over distances of 250–500 km. This lateral variation may explain the paucity of observations and difficulty in measuring the impedance contrast and sharpness of this discontinuity^{1,2,15}.

Numerous investigations of the transitional upper mantle from 200 to 700 km depth have been made over the past fifty years. The thickness and relative velocity contrast of upper mantle discontinuities are best determined from wide-angle P and S waves^{16–18} recorded in the distance range 15° to 30°, near-source^{9,20} and near-receiver^{12,21,22} reflections and conversions, or from PP, SS and P'P' precursors^{1,2,13–15,23–25}.

P'P' (PKPPK), which is best observed in the distance range 65° to 75° with a caustic occurring near 71°, has been widely studied because its precursors (typically under-side reflections from mantle discontinuities) are ideal for identifying and measuring the transitional thickness of such discontinuities. P'P' precursors are commonly labelled as P'_dP' where *d* denotes the depth of the reflector. We will use this convention, and will refer to the three main upper-mantle discontinuities by their average globally observed depths, that is, the 410-, 520- and 660-km discontinuities^{7,11}.

Since the early 1970s, the United States Geological Survey (USGS) and the California Institute of Technology have been operating regional seismic arrays in California (Fig. 1a). These